

Asymptotic Spectral Efficiency of the Uplink in Spatially Distributed Wireless Networks With Multi-Antenna Base Stations

Siddhantan Govindasamy, *Member*, D. W. Bliss, *Senior Member, IEEE*, and David H. Staelin, *Life Fellow, IEEE*

Abstract—The spectral efficiency of a representative uplink of a given length, in interference-limited, spatially-distributed wireless networks with hexagonal cells, simple power control, and multi-antenna linear Minimum-Mean-Square-Error receivers is found to approach an asymptote as the numbers of base-station antennas N and wireless nodes go to infinity. An approximation for the area-averaged spectral efficiency of a representative link (averaged over the spatial base-station and mobile distributions), for Poisson distributed base stations, is also provided. For large N , in the interference-limited regime, the area-averaged spectral efficiency is primarily a function of the ratio of the product of N and the ratio of base-station to wireless-node densities, indicating that it is possible to scale such networks by linearly increasing the product of the number of base-station antennas and the relative density of base stations to wireless nodes, with wireless-node density. The results are useful for designers of wireless systems with high inter-cell interference because it provides simple expressions for spectral efficiency as a function of tangible system parameters like base-station and wireless-node densities, and number of antennas. These results were derived combining infinite random matrix theory and stochastic geometry.

Index Terms—Cellular Networks, MIMO, Antenna Arrays, Stochastic Geometry, Hexagonal Cells.

I. INTRODUCTION

It is increasingly common for multiple wireless networks to be within interfering distance of each other in urban environments today due to proliferation of systems such as city-wide wireless internet access, pico cells for mobile telephony, and wireless local-area networks. Antenna arrays at base stations that employ spatial interference mitigation can significantly increase data rates in such systems. It is thus important to study the spectral efficiencies (b/s/Hz) of wireless links with multiple antennas in environments that have high base station or access point and wireless-node densities. In such systems the densities of nodes (both in-and out-of-cell) and their distribution in space are important factors as they influence inter-node distances and hence signal and interference strengths, which directly impact the Signal-to-Interference-Plus-Noise-Ratio (SINR), spectral efficiency and ultimately data rates.

S. Govindasamy is with the Franklin W. Olin College of Engineering. (email: siddhantan.govindasamy@olin.edu, d.w.bliss@asu.edu, staelin@mit.edu). Daniel W. Bliss is at the School of Electrical, Computer and Energy Engineering at Arizona State University. D. H. Staelin was with the Research Laboratory of Electronics, Massachusetts Institute of Technology (MIT). Opinions, interpretations, conclusions, and recommendations are those of the authors and are not necessarily endorsed by the United States Government. This research was supported in part by the National Science Foundation under Grant ANI-0333902. Portions of this material have appeared in Conference Record of the 42nd Asilomar Conference on Signals, Systems and Computers, October 2008.

Most works on wireless networks with multi-antenna base-stations do not explicitly model out-of-cell interference from spatially distributed in-band interferers which is known to be very challenging. Andrews et al. [1] remark that “despite decades of research, tractable models that accurately model other-cell interference (OCI) are still unavailable, which is fairly remarkable given the size of the industry”.

Several authors have used infinite random matrix theory techniques similar to ours to analyze multi-antenna cellular networks such as Dai and Poor [2] and Couillet et al. [3]. Neither of these works models the spatial distribution of nodes and thus do not capture the effects of interference from users that are spatially distributed. Monte-carlo simulations were used in [4] and [5] to analyze small, spatially-distributed multi-antenna cellular networks. Cellular networks with *single*-antenna base-stations and spatially distributed nodes have been analyzed in works such as [1], [6], and [7] using stochastic geometry to model the spatial distribution of nodes. Further discussion of [1] and [7] which are related to this work are given at the end of this section. Stochastic geometry has also been used to study *ad hoc* wireless networks with both multi and single antenna nodes using both finite and asymptotic techniques in works such as [8], [9] [10], [11], [12] and [13]. Please see [14] for a survey of works utilizing stochastic geometry in both cellular and ad hoc wireless networks and [15] and [16] which present an extensive set of useful stochastic geometry techniques.

In this work, we show that with appropriate normalization, the spectral efficiency of a representative uplink in a network with hexagonal cells, and base-stations with N antennas using the linear MMSE receiver converges in probability and derive an asymptotic expression for the area-averaged spectral efficiency. We use the term area-averaged spectral efficiency to refer to the average spectral efficiency of a link where the averaging is taken over the locations of all the nodes in the network and fading, to distinguish it from the ergodic spectral efficiency in the Shannon sense. Note that the hexagonal-cell model is an idealized model for base-station placement that is commonly used in the literature as it offers the best coverage of the plane if we assume that the coverage associated with each cell is a disk. Furthermore, with a few modifications, we apply the techniques developed for hexagonal cells to derive an approximation to the area-averaged spectral efficiency of a link in a network where base stations are distributed according to a Poisson Point Process (PPP).

We consider interference from spatially distributed in-cell

and out-of-cell wireless nodes that have single antennas and transmit simultaneously in the same channel using distance-dependent power control. We assume that signal power decays with distance according to the standard inverse power-law model. The area-averaged per-link spectral efficiency is expressed as a function of the number of receiver antennas N , wireless-node and base-station densities, and path-loss exponent. While the exact CDF of the spectral efficiency for finite systems would be ideal, computation of this quantity is difficult for the uplink in cellular systems with power-control as the transmit powers of nodes depend on their location on the plane. Moreover for Poisson distributed base stations, the transmit powers of mobile users are dependent, further complicating analysis. We use an asymptotic analysis to handle complexities of the uplink, in particular the dependence of transmit powers of the mobile nodes as described in more detail at the end of this section. The asymptotic techniques also help handle the difficulties in analytically characterizing the hexagonal cell model which is typically viewed as being intractable (as noted in [1], [7]) and are usually analyzed by Monte-carlo simulation such as in [17].

The asymptotic expressions we provide are useful in understanding the behavior of large networks, such as the rate of spectral efficiency growth with the number of antennas and base-station density, and to understand the performance differences between a network with regularly-spaced, and completely random base-station placements.

Of the recent works that apply stochastic geometry to analyze cellular networks, [1] is of particular note as they introduce a framework to analyze cellular networks with Poisson base-station placements. Their work assumes single antenna nodes, exactly one active wireless node per cell, and exclusively focuses on the downlink. In their model, the transmit powers of the base stations are constant allowing them to use a Poisson shot-noise model for the interference which is at the heart of the derivation of their main results. Such an approach is not applicable for the uplink, which is the focus of this work, due to the correlation between transmit powers of wireless nodes that result from power control which is an essential feature of the uplink. The correlation arises because the transmit powers of the wireless nodes are dependent on their positions relative to the base-stations in their respective cells. The size and shape of the cells are of course dependent. This correlation between transmit powers precludes applying standard Poisson techniques which typically require the transmit powers of nodes to be independent of one another.

As noted in a very recent work by Novlan, et al. [7] “the analysis of the uplink requires several fundamental changes as compared to the downlink, nearly all of which make it more challenging.” In [7] which considers single-antenna uplinks in random-cell networks, this complexity is handled by applying certain approximations to the network topology such as approximating the transmit powers of the wireless nodes as independent. They make a further approximation on the base-station distribution by first generating Voronoi cells about the mobile nodes and then placing a base station with uniform probability inside each Voronoi cell. Thus, the base-stations in their model are spatially correlated and not

Poisson. In contrast, in the extension of our results to Poisson-distributed multi-antenna base stations, we assume that cells are formed with the base stations as the generator points as is typically done (e.g. for the downlink in [1]), and that the mobile nodes perform distance-dependent power control which introduces dependence between the transmit powers. The associated complexities are handled by the asymptotic analysis which combines stochastic geometry and infinite random matrix theory. We validated the results for finite systems using Monte Carlo simulations that were also used to characterize the spectral efficiency for a given outage probability.

II. SYSTEM MODEL

Consider a planar wireless network with base stations distributed at hexagonal lattice sites with minimum base-station separation d , with a base-station at the origin. While in practical systems, base-station assignments are based on strongest received signals rather than distance alone, to simplify analysis, the wireless nodes are assumed to communicate with their closest base station in Euclidian distance. In other words we assume that the cells are formed by the Voronoi tessellation of the plane (see e.g. [18]) with the base stations as the generator points.

The base station at the origin is called the *representative receiver* which is in a link with a *representative transmitter* at a distance r_1 away. We shall consider both constant r_1 and random r_1 resulting from the representative transmitter being distributed with uniform probability in the cell associated with the representative receiver. The later case will be called the *random link* case. The link between the two is called the *representative link*. The representative receiver is assumed to have N antennas and the representative transmitter and interferers (to be defined in the next paragraph) have single antennas.

Suppose that there is a circular network of radius R centered at the origin with n additional wireless nodes (in addition to the representative transmitter) distributed in an independent, identically distributed (i.i.d.) fashion in the network with uniform probability such that

$$n = \rho_w \pi R^2, \quad (1)$$

where ρ_w is the effective area density of the wireless nodes which are co-channel interferers to the representative link. Note that these are nodes that are *actively* transmitting in our model so the true density of nodes may be much higher. An example of this network is illustrated in Figure 1. The representative transmitter and interferers are labeled as follows. Node 1 is the representative transmitter, and nodes $2, 3, \dots, n+1$ are the interferers in random order of distance from the origin. The asymptotic regime we consider is the limit as N , R and n are taken to infinity such that $c = n/N > 2$, ρ_w is constant and (1) holds. In the following we assume that whenever $N \rightarrow \infty$, n and $R \rightarrow \infty$ in this manner as well. The resulting network has wireless nodes distributed uniformly randomly on the entire plane with density ρ_w . Note that since we are interested in large wireless networks with moderately large numbers of base-station antennas, $2 \ll c$.

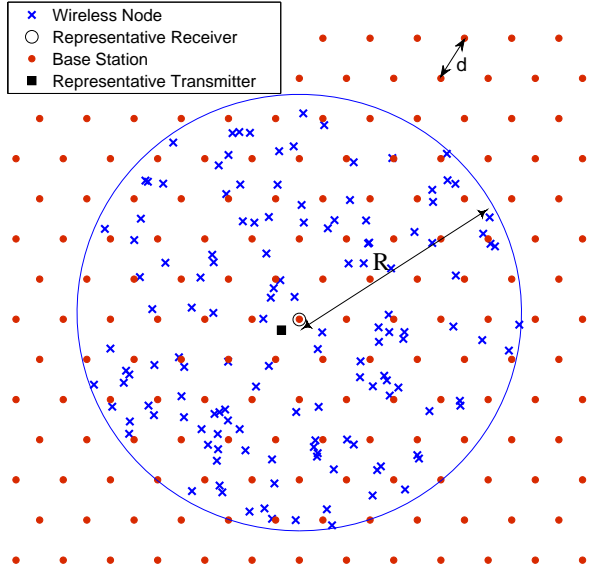


Fig. 1. Illustration of wireless network with representative link and base-stations at hexagonal lattice sites. The representative receiver is at the origin and the representative transmitter is denoted by the filled square. The remaining base stations are represented by the dots and the interfering wireless nodes are represented with the crosses.

The i -th wireless node is at distance r_i from the representative receiver at the origin and is assumed to transmit with power P_i . The average received signal power per antenna (averaged over the fading distribution defined in the next paragraph) due to the i -th wireless node is

$$p_i = P_i G_t r_i^{-\alpha} \quad (2)$$

with the path-loss exponent $\alpha > 2$, and G_t is a proportionality constant. The wireless nodes control their transmit power in order to achieve a target received power relative to path loss at their closest base station, subject to a maximum power constraint, P_M as follows

$$P_i = \min \left(\frac{p_t}{G_t} r_{ti}^\alpha, P_M \right), \quad (3)$$

where r_{ti} is the distance between the i -th wireless node and its closest base station. Let the limiting probability density function (PDF) of P_i be denoted by $f_P(p)$ and $E[P^\frac{2}{\alpha}]$ be its expected value raised to the power $\frac{2}{\alpha}$.

We assume frequency-flat fading with independent, circularly symmetric complex Gaussian channel coefficients between all pairs of antennas. Let $\mathbf{y} \in \mathbb{C}^{N \times 1}$ be the vector of sampled received signals at the N antennas of the representative receiver at a given sampling time, and $\mathbf{w} \in \mathbb{C}^{N \times 1}$ contain zero-mean, i.i.d. complex Gaussian noise terms of variance σ^2 denoted by $\mathcal{CN}(0, \sigma^2)$. This system can be represented by the following equation:

$$\mathbf{y} = \sqrt{p_1} \mathbf{g}_1 x_1 + \sum_{i=2}^{n+1} \sqrt{p_i} \mathbf{g}_i x_i + \mathbf{w} \quad (4)$$

where $\mathbf{g}_i \in \mathbb{C}^{N \times 1}$ has i.i.d. $\mathcal{CN}(0, 1)$ entries and x_i is the transmitted symbol of the i -th wireless node with $E[|x_i|^2] = 1$.

Thus, \mathbf{g}_i captures the Rayleigh fading and p_i captures the combined transmit power and path loss associated with node- i . To focus on the interference-limited regime, we set the noise power $\sigma^2 = 0$.

We assume that the base stations use spatial linear MMSE estimators to mitigate interference. Note that the linear MMSE receiver is the linear receiver that maximizes the SINR (e.g. see [19]) which maximizes the spectral efficiency for Gaussian signals. We assume that all nodes use Gaussian codebooks which results in Gaussian distributed residual interference at the output of the linear MMSE receiver. Thus, the spectral efficiency is given by the Shannon formula as is commonly done in the literature (e.g. [1]). It is important to note here that the rapid decay of signal power with distance associated with the inverse power-law path-loss model means that the central-limit theorem does not hold for a general distribution of transmit signals (e.g. Quadrature-Amplitude-Modulation [20]). Thus the aggregate interference at the *input* to the MMSE receiver will not be Gaussian distributed (e.g. see [20]) if the transmitted signals themselves are not Gaussian to begin with. If we do not make the assumption that the transmitted signals are Gaussian distributed, the spectral efficiencies we compute should be interpreted as *achievable* spectral efficiencies because the Gaussian distribution is entropy maximizing. Thus from an information theoretic perspective, the spectral efficiency obtained by assuming a Gaussian interference distribution is a lower bound to the spectral efficiency achievable with any other interference distribution. Additionally, it is common practice to design systems to operate in Gaussian noise. One could apply a correction factor, η say, to the SIR and compute the spectral efficiency as $\log_2(1 + \eta \text{SIR})$. This has been suggested in [1] and other works. While we do not use a scale factor of η here, introducing it into our expressions is straightforward.

The main results of this work will be given in terms of a normalized version of the Signal-to-Interference-Ratio (SIR),

$$\beta_N = N^{-\frac{\alpha}{2}} \mathbf{g}_1^\dagger \left(\sum_{i=2}^{n+1} p_i \mathbf{g}_i \mathbf{g}_i^\dagger \right)^{-1} \mathbf{g}_1 \quad \text{for which} \quad (5)$$

$$\text{SIR} = p_1 N^{\frac{\alpha}{2}} \beta_N. \quad (6)$$

Note that up to the normalization by $N^{-\alpha/2}$, (5) is the standard equation for the SINR associated with a linear MMSE receiver with the noise variance assumed to equal zero, as we have assumed here. This assumption is used in order to utilize an asymptotic approach to characterize interference-limited systems. We make the additional observation here that although we assume zero noise, the resulting receiver does not reduce to a zero-forcing receiver as the number of antennas N is less than the number of interferers since $c = n/N > 2$ by assumption. This means that the degrees of freedom at the receiver are insufficient to force the interference to zero.

Note that the normalization of the SIR by $N^{\frac{\alpha}{2}}$ keeps the SIR finite as $N \rightarrow \infty$ because the SIR grows as $N^{\frac{\alpha}{2}}$. This order of growth of the SIR with the number of antennas in networks with the inverse-power-law path-loss model is known and can be interpreted intuitively as is done for ad hoc networks in [10], or using a precise analysis as done in [11]. Based on

our description in [10], note that the representative receiver can use a fraction of its degrees of freedom to null nearby interferers who occupy a disk of radius on the order of \sqrt{N} around the representative receiver. The aggregate interference from the un-nulled interferers outside this disk is of order $N^{\alpha/2-1}$. The remaining fraction of the degrees of freedom are used to add signals from the target transmitter coherently, increasing signal power relative to interference by a factor on the order of N . The combined effect is that the SIR grows as a factor of $N^{\alpha/2}$.

III. MAIN RESULTS

The main results of this work are based on the following theorem proved in Appendix A using Lemma 1 which follows.

Theorem 1: Consider the network model from Section II. As $N, n, R \rightarrow \infty$, the normalized SIR, β_N converges in probability to a limit β which is the unique non-negative solution to the following equation

$$E[P^{\frac{2}{\alpha}}] \beta^{\frac{2}{\alpha}} \left[\frac{\pi}{\alpha} \csc \left(\frac{2\pi}{\alpha} \right) \right] - \frac{2\pi\rho_w\beta}{\alpha} \times \int_0^\infty \frac{\tau^{-\frac{2}{\alpha}}}{1+\tau\beta} \int_{\tau/b}^\infty f_P(x) x^{\frac{2}{\alpha}} dx d\tau = \frac{1}{2\rho_w\pi} \quad (7)$$

where $b = \left(\frac{\pi\rho_w}{c} \right)^{\frac{\alpha}{2}}$.

Lemma 1: Consider the quantity

$$\gamma_N = \frac{1}{N} \mathbf{s}^\dagger \left(\frac{1}{N} \mathbf{S} \mathbf{\Psi} \mathbf{S}^\dagger \right)^{-1} \mathbf{s} \quad (8)$$

where $\mathbf{s} \in \mathbb{C}^{N \times 1}$ and $\mathbf{S} \in \mathbb{C}^{N \times n}$ comprise i.i.d., zero-mean, unit-variance entries from a continuous distribution, $n/N = c$, and $\mathbf{\Psi} = \text{diag}(\psi_2, \psi_3, \dots, \psi_{n+1})$. Note that $\mathbf{R} = \frac{1}{N} \mathbf{S} \mathbf{\Psi} \mathbf{S}^\dagger$ is invertible with probability 1 (w.p.1) since $N < n$. Suppose that as $n, N \rightarrow \infty$, the empirical distribution function (e.d.f.) of the diagonal entries of $\mathbf{\Psi}$ converges w.p.1 to a function $H(x)$. Additionally, assume that there exists an N_0 such that $\forall n > N_0$, the minimum eigenvalue of \mathbf{R} is bounded from below by $\lambda_{\ell b} > 0$, w.p.1. Then, $\gamma_N \rightarrow \gamma$ in probability where γ is given by the non-negative real solution for m in

$$1 = m c \int_0^\infty \frac{\tau dH(\tau)}{1+\tau m}. \quad (9)$$

Proof: Please see Appendix B.

Note that Lemma 1 is closely related to several results in the literature concerning the convergence of the SINR of random Direct/Sequence Code-Division-Multiple-Access (DS/CDMA) systems such as [19] and [21]. The existing results however assume that the noise power is strictly positive and are thus not directly applicable to systems with negligible noise power. Lemma 1 is proved by modifying the proof in [19], replacing the requirement of the strictly positive noise by the requirement on the minimum eigenvalue of the matrix \mathbf{R} .

Since we assume that all nodes use Gaussian codebooks which results in Gaussian residual interference at the output of the MMSE receiver, we can approximate the per-link spectral

efficiency using the Shannon formula assuming that the noise is negligible as follows.

$$C(r_1) = \log_2(1 + \text{SIR}) = \log_2(1 + N^{\frac{\alpha}{2}} P_1 r_1^{-\alpha} \beta_N),$$

where we emphasize that the spectral efficiency is a function of the length of the representative link, r_1 . Note that if the transmit signals are not Gaussian, as we noted in the system model, the spectral efficiency above and in subsequent expressions should be interpreted as achievable spectral efficiencies.

Since the log function is continuous, as $N \rightarrow \infty$ $\beta_N \rightarrow \beta$ and,

$$C(r_1) - \log_2(N^{\frac{\alpha}{2}}) \rightarrow \log_2(P_1 r_1^{-\alpha} \beta), \quad (10)$$

in probability (e.g. see [22]). Hence, with appropriate normalization, the spectral efficiency approaches an asymptote as $N \rightarrow \infty$. We define this asymptotic spectral efficiency as $C^*(r_1) = \log_2(1 + N^{\frac{\alpha}{2}} P_1 r_1^{-\alpha} \beta)$.

While β is given implicitly by Theorem 1¹ and has to be solved numerically, we can approximate the spectral efficiency of a system where the number of interferers n greatly exceeds the number of base-station antennas N , i.e. small b because the second term on the LHS of (7) is small in this case. In fact this term can be shown to go to zero as $b \rightarrow 0$ (after the limits on n, N and R are taken) [10]. Writing $G_\alpha = \left[\frac{\alpha}{2\pi} \sin \left(\frac{2\pi}{\alpha} \right) \right]^{\frac{\alpha}{2}}$, this yields the following approximation

$$C^*(r_1) \approx \log_2 \left(1 + N^{\frac{\alpha}{2}} P_1 G_\alpha \left(\frac{1}{E[P^{\frac{2}{\alpha}}] \pi \rho_w r_1^2} \right)^{\frac{\alpha}{2}} \right). \quad (11)$$

Applying the dominated convergence theorem with steps similar to that in Appendix E of [23] with the noise power replaced by $\lambda_{\ell b}$ we can show that

$$E[C|r_1] - C^*(r_1) \rightarrow 0. \quad (12)$$

Hence the asymptotic spectral efficiency C^* is a good approximation for the conditional area-averaged spectral efficiency $E[C|r_1]$ (averaging is over wireless-node locations and fading distributions here) for large N . Finally, we can find the unconditioned area-averaged spectral efficiency of a random link by averaging with respect to the distribution of r_1 so that

$$E[C] \approx \int C(r_1) f_{r_1}(r) dr, \quad (13)$$

where $f_{r_1}(r)$ is the PDF of r_1 which equals $f_X(x)$ given in Lemma 2.

If the minimum distance between base stations $d \leq \frac{3}{\sqrt{3}} \left(\frac{G_t P_M}{p_t} \right)^{\frac{1}{\alpha}}$, the cells are small enough that all wireless nodes have sufficient transmit power to meet the target received power p_t at their base-stations. We call this the sufficient-power case in which the asymptotic spectral efficiency takes a simple form which is independent of whether

¹To the best of our knowledge, the only scenario in which similar techniques have resulted in closed form solutions are when the received interference powers from all users are equal [19]

r_1 is fixed or random due to the power control. Substituting the power control equation (3) into (11)

$$E[C] \approx C^*(r_1)$$

$$\approx \log_2 \left(1 + \frac{p_t}{G_t} r_1^\alpha G_\alpha \left(\frac{N}{E \left[\left(\frac{p_t}{G_t} r_{ti}^\alpha \right)^{\frac{2}{\alpha}} \right] \pi \rho_w r_1^2} \right)^{\frac{\alpha}{2}} \right) \quad (14)$$

$$= \log_2 \left(1 + G_\alpha \left(\frac{N}{E[r_{ti}^2] \pi \rho_w} \right)^{\frac{\alpha}{2}} \right), \quad (15)$$

which is a function of the second moment of the distance between a random wireless node and its closest base station $E[r_{ti}^2]$, wireless-node density ρ_w , number of antennas N and path-loss exponent. $E[r_{ti}^2]$ can be found using the following lemma that statistically characterizes the distance between a random wireless node and its closest base station.

Lemma 2: The PDF $f_X(x)$, CDF $F_X(x)$, and k -th moment of the link length x between a randomly located wireless node and its closest base station in a hexagonal-cellular system with minimum base-station separation d are the following:

$$f_X(x) = \begin{cases} \frac{4\pi}{\sqrt{3}d^2}x, & \text{if } 0 < x < \frac{d}{2} \\ \frac{4\pi}{\sqrt{3}d^2}x - \frac{8\sqrt{3}x}{d^2} \cos^{-1}\left(\frac{d}{2x}\right), & \text{if } \frac{d}{2} < x < \frac{\sqrt{3}d}{3} \\ 0, & \text{otherwise.} \end{cases} \quad (16)$$

$$F_X(x) = \begin{cases} 0, & \text{if } x < 0, \\ \frac{2\sqrt{3}\pi x^2}{3d^2}, & \text{if } 0 \leq x < \frac{d}{2} \\ \frac{2\sqrt{3}\pi x^2}{3d^2} - \frac{4\sqrt{3}x^2}{d^2} \cos^{-1}\left(\frac{d}{2x}\right) + 2\sqrt{3}\left(\frac{x^2}{d^2} - \frac{1}{4}\right)^{\frac{1}{2}}, & \text{if } \frac{d}{2} \leq x < \frac{\sqrt{3}d}{3} \\ 1, & \text{if } x \geq \frac{\sqrt{3}d}{3}. \end{cases} \quad (17)$$

$$E(x^k) = \frac{2\sqrt{3}}{k+2} \left(\frac{d}{2}\right)^k \int_0^{\frac{\pi}{6}} \frac{1}{(\cos \tau)^{k+2}} d\tau. \quad (18)$$

Proof: Consider Figure 2 which illustrates a portion of a wireless network with hexagonal cells. Each wireless node in the network falls on some random point in an equilateral triangle formed by the three base stations closest to it, and forms a link with the base station at the closest vertex of that triangle as illustrated in Figure 2. Thus, the link-lengths are statistically equivalent to the distance between a randomly selected point in an equilateral triangle to the closest vertex of that triangle. The CDF, PDF and k -th moments of the distance between a random point in an equilateral triangle to the closest vertex are known [24], and are precisely the formulae in Lemma 2. Note that the PDF of link-lengths associated with a hexagonal cell which equals (16), has been given without proof before in [25]. ■

From (15), the spectral efficiency depends on the second moment of link-lengths given by (18) with $k = 2$.

$$E[t_{ti}^2] = \frac{5}{36}d^2 \approx 0.14d^2.$$

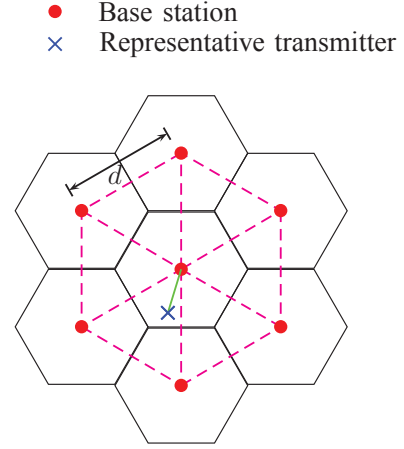


Fig. 2. Illustration of base stations at hexagonal lattice sites.

Substituting into (15) yields the following approximation for the area-averaged and asymptotic uplink spectral efficiency of a random link (as defined in Section II), in interference-limited, hexagonal-cell systems with a large number of base-station antennas and high transmit power budgets:

$$E[C] \approx C^*(r_1) \approx \log_2 \left(1 + G_\alpha \left(\frac{36 N}{5 d^2 \pi \rho_w} \right)^{\frac{\alpha}{2}} \right). \quad (19)$$

In terms of the effective density of base stations from the hexagonal-cell model ρ_h we can write,

$$E[C] \approx C^*(r_1) \approx \log_2 \left(1 + G_\alpha \left(\frac{1.98 N \rho_h}{\rho_w} \right)^{\frac{\alpha}{2}} \right). \quad (20)$$

If $d > \frac{3}{\sqrt{3}} \left(\frac{G_t P_M}{p_t} \right)^{\frac{1}{\alpha}}$, the transmit power budget is insufficient for all nodes to meet the target received power at their base stations which results in some wireless nodes transmitting at full power. In this case, $E[P_\alpha^{\frac{2}{\alpha}}]$ is given by the following lemma which can be proved by direct computation using Lemma 2:

Lemma 3: If $P_M < \frac{p_t}{G_t} \left(\frac{d}{2}\right)^\alpha$,

$$E[P_\alpha^{\frac{2}{\alpha}}] = P_M^{\frac{2}{\alpha}} - \frac{\sqrt{3}\pi}{3d^2} \left(\frac{G_t}{p_t} \right)^{\frac{2}{\alpha}} P_M^{\frac{4}{\alpha}}. \quad (21)$$

If $\frac{p_t}{G_t} \left(\frac{d}{2}\right)^\alpha \leq P_M < \frac{p_t}{G_t} \left(\frac{\sqrt{3}d}{3}\right)^\alpha$,

$$E[P_\alpha^{\frac{2}{\alpha}}] = P_M^{\frac{2}{\alpha}} - \frac{\pi\sqrt{3}}{3d^2} \left(\frac{p_t}{G_t} \right)^{-\frac{2}{\alpha}} P_M^{\frac{4}{\alpha}} + \frac{2\sqrt{3}}{d^2} \left(\frac{p_t}{G_t} \right)^{-\frac{2}{\alpha}} P_M^{\frac{4}{\alpha}} \cos^{-1} \left(\frac{d}{2} \left(\frac{p_t}{G_t P_M} \right)^{\frac{1}{\alpha}} \right) + \left(\frac{\sqrt{3}d}{12} \left(\frac{p_t}{G_t} \right)^{\frac{2}{\alpha}} - \frac{5\sqrt{3}}{6d} P_M^{\frac{2}{\alpha}} \right) \sqrt{4 \left(\frac{G_t P_M}{p_t} \right)^{\frac{2}{\alpha}} - d^2}. \quad (22)$$

Lemma 3 substituted into (11) yields the area-averaged spectral efficiency for a length r_1 link.

Averaged over the PDF of link-lengths arising from hexagonal cells (i.e., the representative transmitter is distributed with

$$\begin{aligned}
E[C] &\approx \int_0^{r_t} \log_2 \left(1 + G_\alpha \frac{p_t}{G_t} x^\alpha \left(\frac{N}{E[P_\alpha^2] \pi \rho_w x^2} \right)^{\frac{\alpha}{2}} \right) f_X(x) dx + \int_{r_t}^{\frac{\sqrt{3}d}{3}} \log_2 \left(1 + G_\alpha P_M \left(\frac{N}{E[P_\alpha^2] \pi \rho_w x^2} \right)^{\frac{\alpha}{2}} \right) f_X(x) dx \\
&= F_X(r_t) \log_2 \left(1 + G_\alpha \frac{p_t}{G_t} \left(\frac{N}{E[P_\alpha^2] \pi \rho_w} \right)^{\frac{\alpha}{2}} \right) + \int_{r_t}^{\frac{\sqrt{3}d}{3}} \log_2 \left(1 + G_\alpha P_M \left(\frac{N}{E[P_\alpha^2] \pi \rho_w x^2} \right)^{\frac{\alpha}{2}} \right) f_X(x) dx
\end{aligned} \tag{24}$$

uniform probability in the cell containing the origin), the area-averaged spectral efficiency of a random link is given by (24) at the top of this page, where we have used $r_t = \left(\frac{p_t}{P_M G_t} \right)^{-\frac{1}{\alpha}}$, $F_X(x)$ and $f_X(x)$ from Lemma 1, and $E[P_\alpha^2]$ is from Lemma 3. We were not able to integrate the second term on the RHS of (24) in closed form and thus use numerical integration to compute it.

IV. EXTENSION TO POISSON DISTRIBUTED BASE STATIONS

A. Area-averaged Spectral Efficiency

The results for the hexagonal-cell model can be extended to a *Poisson-cell* model where base stations are distributed according to a homogenous PPP with density ρ_t , conditioned on there being a point of the PPP at the origin. We denote the conditioned PPP by PPP^o . Conditioned on a realization of the base-station locations Π_t , Theorem 1 still holds if $E[P_\alpha^2]$ and $f_P(p)$ are replaced with $E[P_\alpha^2 | \Pi_t]$ and $f_{P|\Pi_t}(p | \Pi_t)$ respectively.

The ergodicity of the PPP however implies that $E[P_\alpha^2 | \Pi_t]$ is equal for almost all realizations of Π_t (i.e. any deviations occur with probability zero). Similarly, $f_{P|\Pi_t}(p | \Pi_t)$ is equal for almost all realizations of Π_t . These properties and the expressions for $E[P_\alpha^2 | \Pi_t]$ and $f_{P|\Pi_t}(p | \Pi_t)$ are given explicitly in the following lemma.

Lemma 4: With probability 1,

$$\begin{aligned}
E[P_\alpha^2 | \Pi_t] &= \left(\frac{p_t}{G_t} \right)^{\frac{2}{\alpha}} \frac{1 - e^{-\pi \rho_t \left(\frac{G_t}{p_t} P_M \right)^{\frac{2}{\alpha}}}}{\pi \rho_t} \\
&= E[P_\alpha^2] = E[P_\alpha^2 | \Pi_t, r_1].
\end{aligned} \tag{25}$$

and

$$\begin{aligned}
f_{P|\Pi_t}(p | \Pi_t) &= f_{P|\Pi_t, r_1}(p | \Pi_t, r_1) = \\
f_P(p) &= \begin{cases} \frac{2\rho_t \pi}{\alpha p} \left(\frac{p G_t}{p_t} \right)^{\frac{2}{\alpha}} e^{-\rho_t \pi \left(\frac{p G_t}{p_t} \right)^{\frac{2}{\alpha}}}, & \text{if } p \leq P_M \\ 0, & \text{otherwise.} \end{cases}
\end{aligned} \tag{26}$$

Proof: In Appendix C.

Thus, the solution for β in Theorem 1 takes a fixed value for almost all realizations of Π_t . From (12) the area-averaged spectral efficiency conditioned on Π_t and r_1 , $E[C | \Pi_t, r_1]$, has the following property w.p.1 as $n, N, R \rightarrow \infty$.

$$E[C | \Pi_t, r_1] - \log_2(1 + P_1 r_1^{-\alpha} N^{\alpha/2} \beta) \rightarrow 0, \tag{27}$$

where β is the non-negative solution to (7) with $E[P_\alpha^2]$ and $f_P(p)$ from Lemma 4. Removing the conditioning with respect to r_1 and Π_t yields the following property of the area-averaged spectral efficiency $E[C]$ (where the averaging is over the

fading and wireless-node locations, base-station locations and representative link length), as $n, N, R \rightarrow \infty$

$$E[C] - \int \log_2(1 + P_1 r_1^{-\alpha} N^{\alpha/2} \beta) f_{r_1}(r_1) dr_1 \rightarrow 0, \tag{28}$$

where we have used the fact that β equals the same value over almost all realizations of Π_t , and the monotone convergence theorem (see e.g. [22]) to exchange the limit and expectation.

Although β has to be found numerically in general, by assuming that $c = n/N$ is large, as done in Section III, the area-averaged spectral efficiency conditioned on r_1 is approximated from (27) as follows

$$E[C | \Pi_t, r_1] \approx \log_2 \left(1 + G_\alpha P_1 \left(\frac{N}{E[P_\alpha^2] \pi \rho_w r_1^2} \right)^{\frac{\alpha}{2}} \right) \tag{29}$$

which holds with probability 1. Furthermore, if $\frac{p_t}{G_t} r_1^\alpha < P_M$, i.e., the transmit power budget is sufficient for the representative transmitter to achieve the target received power p_t at the representative base station, substituting (3) and (25) into (29) yields the following approximation which holds with probability 1.

$$\begin{aligned}
E[C | \Pi_t, r_1] &\approx \\
&\log_2 \left(1 + G_\alpha \left(\frac{\rho_t N}{\left(1 - e^{-\pi \rho_t \left(\frac{G_t}{p_t} P_M \right)^{\frac{2}{\alpha}}} \right) \rho_w} \right)^{\frac{\alpha}{2}} \right)
\end{aligned} \tag{30}$$

With probability 1, the above expression approximates the area-averaged spectral efficiency of a wireless link that has a sufficient power budget to meet its target received power where the average is taken over the fading and wireless-node distributions. If we further assume that the transmit power budget P_M is large, the exponential term in the expression above is small, resulting in the following simple expression for the area-averaged spectral efficiency which holds with probability 1.

$$E[C | \Pi_t] \approx \log_2 \left(1 + G_\alpha \left(\frac{N \rho_t}{\rho_w} \right)^{\frac{\alpha}{2}} \right) \approx E[C]. \tag{31}$$

Note that the approximation above holds with probability 1 and is essentially not dependent on the specific realization of Π_t as a consequence of the ergodicity of the PPP and the large number of degrees of freedom at the MMSE receiver, which makes the system less sensitive to variations in the base-station positions. Additionally, note that the area-averaged spectral efficiency from (31) primarily depends on ρ_t / ρ_w , implying

$$E[C] \approx \int_0^\infty \log_2 \left(1 + \min \left(\frac{p_t}{G_t} r_1^\alpha, P_M \right) r_1^{-\alpha} G_\alpha \left(\frac{N}{E[P_\alpha^2] \pi \rho_w} \right)^{\frac{\alpha}{2}} \right) 2\pi \rho_t r_1 e^{-\pi \rho_t r_1^2} dr_1 = \left(1 - e^{-\pi \rho_t \left(\frac{G_t}{P_M} \right)^{\frac{2}{\alpha}}} \right) \times \log_2 \left(1 + \frac{p_t}{G_t} G_\alpha \left(\frac{N}{E[P_\alpha^2] \pi \rho_w} \right)^{\frac{\alpha}{2}} \right) + \int_{r_t}^\infty \log_2 \left(1 + P_M r_1^{-\alpha} G_\alpha \left(\frac{N}{E[P_\alpha^2] \pi \rho_w} \right)^{\frac{\alpha}{2}} \right) 2\pi \rho_t r_1 e^{-\pi \rho_t r_1^2} dr_1. \quad (32)$$

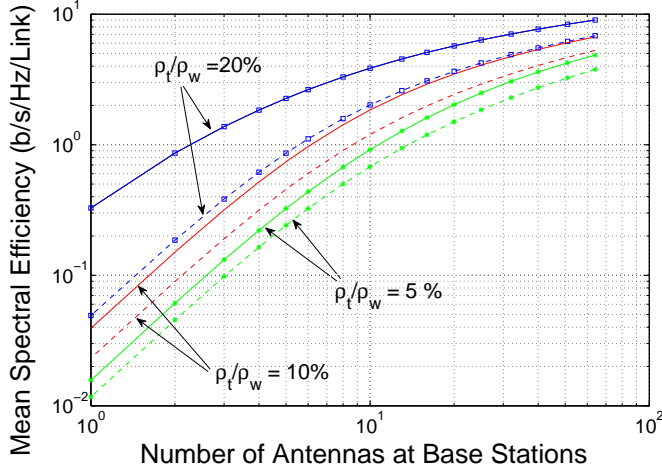


Fig. 3. Area-averaged spectral efficiency of the uplink with random cells and hexagonal cells and transmit power limited to 200 mW. Solid and dashed lines represent hexagonal and random cell asymptotic spectral efficiencies respectively. ρ_t and ρ_w are the base station and wireless node density respectively.

approximate scale invariance in networks where the power budget P_M is not a significant limitation. The scale invariance indicates that as with hexagonal cells (from equation (20)), approximately constant area-averaged spectral efficiency can be maintained by fixing the relative density of base stations to interferers. If the transmit power budgets P_M are not sufficiently large to permit the approximations in (31), we can use (28) with the approximation for β and by observing that r_1 follows the nearest neighbor distribution for Poisson point processes [18] as follows

$$f_{r_1}(r_1) = 2\pi \rho_t r_1 e^{-\pi \rho_t r_1^2} \text{ for } r_1 > 0. \quad (33)$$

The area-averaged spectral efficiency of a random link averaged over realizations of Π_t can then be found by removing the conditioning on r_1 and Π_t by substituting (3) into (29) and integrating with respect to the density in (33) which yields (32) at the top of this page. We were unable to find a closed form expression for the second term on the RHS of (32) and thus use numerical integration to evaluate it.

B. Comparison Between Random and Hexagonal Cells

For systems with limited transmit powers, we numerically evaluated and plotted equations for the spectral efficiency corresponding to random and hexagonal cells in Figure 3, where the solid and dashed lines represent hexagonal and random cells respectively. The transmit power budget was 200 mW and wireless-node density was 10^{-3} with different relative density

of base stations to active interferers as shown in the plot. Note that the difference in area-averaged spectral efficiencies diminishes with the number of antennas. However, for high base-station densities the area-averaged spectral efficiency for random cells is significantly lower. For instance, with 10 antennas at the base stations and 20% relative density of base stations to wireless nodes, the area-averaged spectral efficiency with hexagonal cells is twice that of random cells.

When compared to the area-averaged spectral efficiency with random cells given by (31), (20) indicates that several-fold (but not orders of magnitude) gains in area-averaged spectral efficiency can be achieved by regularly distributing base stations in planar networks compared to randomly distributing them, and furthermore, the difference diminishes with the number of base-station antennas. In practical systems, designers will of course not have the flexibility of placing base stations and mobile user distributions are not uniformly random (i.e. without spatial correlations). Nevertheless, this result sheds some light into the performance differences between these two idealized models which are commonly used in the research community.

V. MONTE CARLO SIMULATIONS

A. Hexagonal Cells

To verify the asymptotic results of the previous section, we simulated network topologies with base stations at hexagonal lattice sites, and interferers distributed randomly on a large circular network on the plane. We simulated each configuration 5000 times. The representative transmitter was placed with uniform probability in the center-most cell.

For each trial, we placed 4000 interferers randomly in circular networks with radii selected to meet target wireless-node densities of 10^{-2} , 10^{-3} , and 10^{-4} nodes m^{-2} . The circular network was overlayed on a hexagonal grid of base stations which extends beyond the edge of the circular network of interferers. The base stations were spaced such that their densities were 20%, 10%, 5% and 2.5% of the wireless-node density. We simulated systems with both unlimited transmit powers (to simulate the sufficient-power case) and powers limited to $P_M = 200mW$.

The channel coefficient between the antenna of wireless node i and antenna j of the representative base station was modeled as $\sqrt{G_t r_i^{-\alpha}} g_{ij}$, where $\alpha = 4$, $G_t = 10^{-5} m^4$, and g_{ij} are i.i.d. $\mathcal{CN}(0, 1)$ random variables which represents the narrow-band Rayleigh fading channel.

1) *Sufficient Transmit Powers*: Figure 4 illustrates the area-averaged uplink spectral efficiency for wireless-node densities of $\rho_w = 10^{-3}$ and $\rho_w = 10^{-2}$ nodes m^{-2} , and unlimited

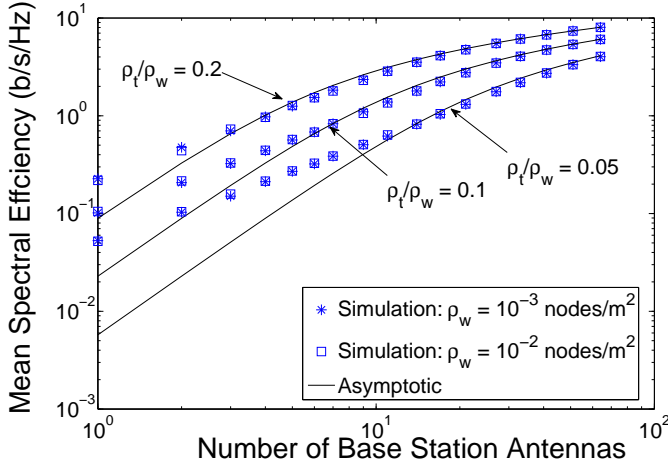


Fig. 4. Area-averaged spectral efficiency vs. number of receive antennas for wireless-node densities of $\rho_w = 10^{-3}$ and $\rho_w = 10^{-2}$ nodes m^{-2} with unlimited transmit powers and hexagonal cells with base-station density of ρ_t .

transmit powers per node versus the number of antennas at the representative base station. The square and asterisk markers represent wireless-node densities of 10^{-2} , and 10^{-3} nodes m^{-2} , respectively and the solid lines represent the asymptotic area-averaged spectral efficiency from (19).

Note that the asterisk and square markers coincide indicating that the absolute density of interferers does not effect the area-averaged spectral efficiency appreciably, and it is the relative density of interferers to base stations that matters. Furthermore, note that the asymptotic approximation (24) holds when N is sufficiently large. When the base-station density is 20% of the *active* wireless-node density, the asymptotic and simulated area-averaged spectral efficiency differ by less than 10% when $N \geq 10$. For lower densities of base stations, the convergence is slower, e.g. when the base-station density is 5% of the active wireless-node density, the difference between the simulated and asymptotic area-averaged spectral efficiency drops below 10% only when $N > 37$.

We analyzed the outage spectral efficiencies from the simulated data, where spectral efficiency with outage probability P_o means that a fraction $1 - P_o$ of the links in our simulations achieved that spectral efficiency or greater. Figure 5 illustrates the outage spectral efficiencies vs. number of receive antennas on the representative link for $\rho_w = 10^{-2}$ nodes m^{-2} with 5%, 25% and 50% outage probabilities. Note that the intersection of the line with the circular markers and the $1 \text{ bs}^{-1} \text{ Hz}^{-1}$ mark in Figure 5 occurs approximately at $N = 14$ indicating that it is possible for 95% of links to achieve $1 \text{ bs}^{-1} \text{ Hz}^{-1}$ with $N \geq 14$ when the base-station density is 10% of the density of *transmitting* interferers. In real systems, the number of nodes transmitting at any time is far smaller than the total number of nodes in the network. Suppose that at any one time, 10% of nodes are actively transmitting in the network. Figure 5 indicates that with a base-station density equaling 1% of total wireless-node density (including inactive ones), it is possible for 95% of links to achieve $1 \text{ bs}^{-1} \text{ Hz}^{-1}$ with 14 antennas at

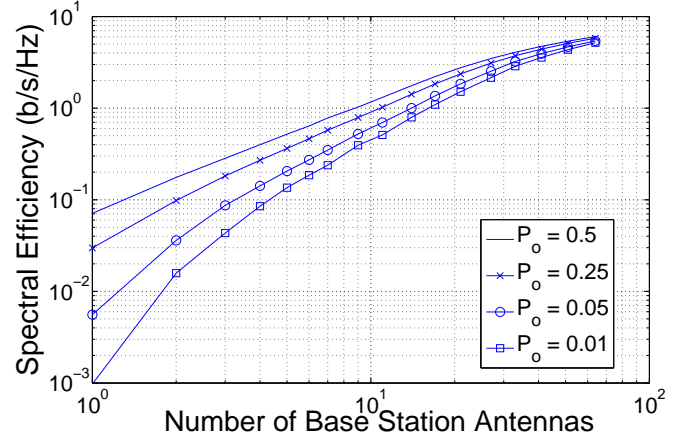


Fig. 5. Outage spectral efficiency vs. number of receive antennas for wireless-node densities of $\rho_w = 10^{-2}$ nodes m^{-2} with unlimited transmit powers and base-station density equaling 10% of wireless-node density, with hexagonal cells.

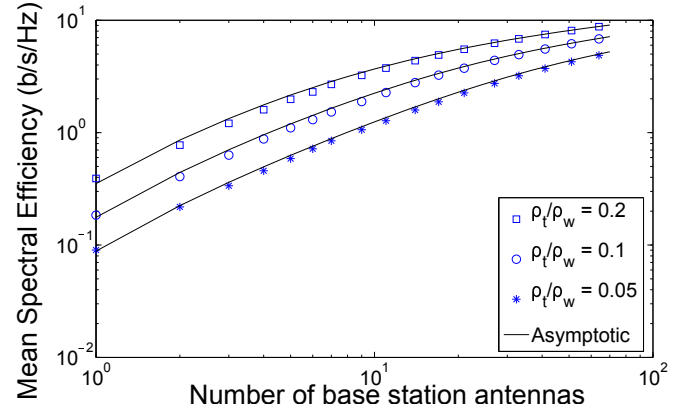


Fig. 6. Area-averaged spectral efficiency for $\rho_w = 10^{-4}$ nodes m^{-2} with different relative density of base station to interferers and hexagonal cells, and 200mW transmit power limits per wireless node.

each base station.

2) *Insufficient Transmit Power*: Figures 6 and 7 illustrate the area-averaged spectral efficiency vs. number of receive antennas for $\rho_w = 10^{-4}$ and $\rho_w = 10^{-2}$ respectively, with $P_M = 200 \text{ mW}$. The markers represent the simulated area-averaged spectral efficiencies for different relative densities of base stations to interferers. The solid lines are the predicted asymptotic area-averaged spectral efficiencies obtained by numerically evaluating equation (24).

It is clear from Figures 6 and 7 that the asymptotic approximation (24) holds when N is sufficiently large. In Figure 6, the simulated and asymptotic area-averaged spectral efficiencies agree to within 5% for $N \geq 2$ for all the base-station densities considered. In Figure 7 however, for base-station densities that are 5% of the wireless-node density of 10^{-2} nodes m^{-2} , the simulated and asymptotic spectral efficiencies differ by less than 13% only when there are 13 or more antenna elements at the receiver. For base-station densities that are 20% of the wireless-node density, the simulated and asymptotic spectral efficiencies agree to within 13% when $N \geq 3$.

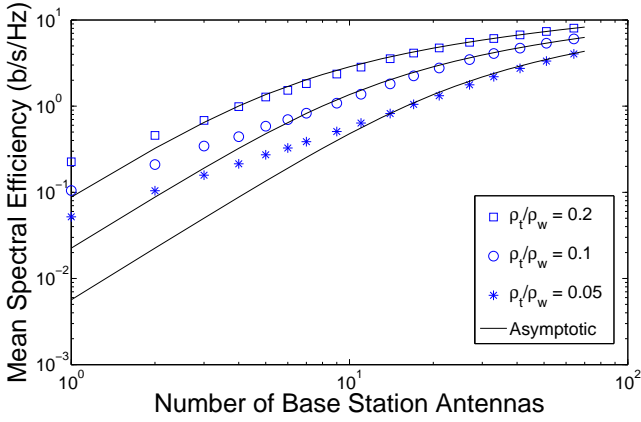


Fig. 7. Area-averaged spectral efficiency vs. number of receive antennas for $\rho_w = 10^{-2}$ nodes m^{-2} with different relative density of base stations to interferers and hexagonal cells, and 200mW transmit power limits per wireless node.

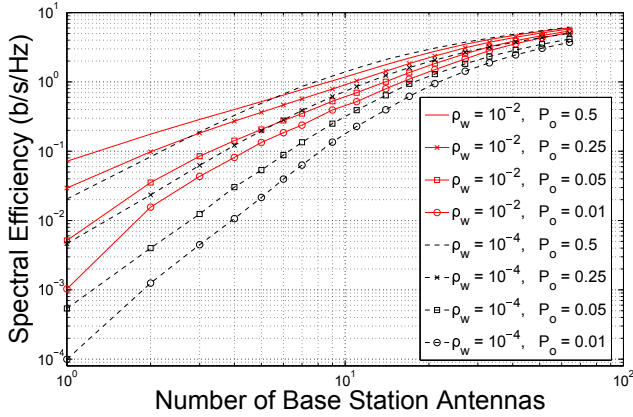


Fig. 8. Outage spectral efficiency vs. number of receive antennas for wireless-node density $\rho_w = 10^{-4}$ and 10^{-2} nodes m^{-2} and base-station density equal to 10% of wireless-node density, hexagonal cells and 200mW transmit power budget. The solid lines represent $\rho_w = 10^{-2}$ and dashed lines represent $\rho_w = 10^{-4}$. The markers represent the different outage probabilities, P_o shown in the legend.

At low wireless-node densities, the simulated spectral efficiencies converge more rapidly (compared to high densities) to the asymptote because a larger fraction of nodes transmit at the power limit. The e.d.f. of interference powers at the representative receiver thus converges more rapidly to its asymptotic value. The rate of convergence of the e.d.f. of interference powers controls the rate of convergence of the eigenvalues of the spatial interference covariance matrix $\sum_{i=2}^{n+1} p_i \mathbf{g}_i \mathbf{g}_i^\dagger$ (see Appendix A and Section 3 of [26]) which affects the convergence rates of the normalized SIR and spectral efficiency.

Figure 8 shows the outage and area-averaged spectral efficiencies for $\rho_w = 10^{-4}$ (solid lines) and $\rho_w = 10^{-3}$ (dashed lines) nodes m^{-2} , 10% relative density of base-stations to interferers and $P_M = 200mW$. Note that with 10 antennas at the receiver, area-averaged spectral efficiencies of approximately 0.2 and 0.3 b/s/Hz are possible for $\rho_w = 10^{-4}$

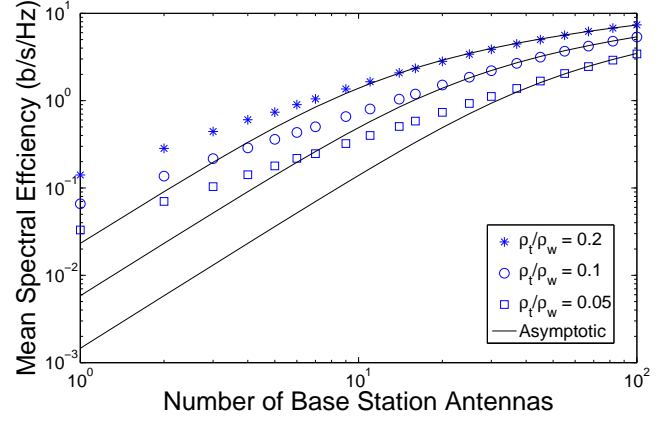


Fig. 9. Area-averaged spectral efficiency of uplink communications with random cells and unlimited transmit powers. Wireless-node density $\rho_w = 10^{-3}$ nodes m^{-2} , $p_t = 10^{-14}$ and $G_t = 10^{-5}$.

and $\rho_w = 10^{-3}$ respectively. The discrepancy in the spectral efficiency is a result of the maximum transmit power. For $\rho_w = 10^{-4}$, a larger fraction of nodes transmit at P_M compared to $\rho_w = 10^{-3}$, resulting in higher SIRs for $\rho_w = 10^{-4}$. The higher total interference power for $\rho_w = 10^{-3}$ is offset by increased signal powers due to shorter links since the relative base-station to wireless-node density is fixed.

B. Poisson Cell Model

We verified (32) and (31) by Monte Carlo simulations of the network topology. We placed base stations in a circular network of radius $4R$. The numbers of base stations were selected to achieve relative densities of base stations to interferers of 20%, 10% and 5%. The network of base stations was then re-centered such that a base-station is at the origin. 4000 interferers were then placed in a circular network of radius R , centered on the base station at the origin with R selected to achieve a wireless-node density of 10^{-3} nodes m^{-2} . This experiment was repeated 1000 times. For each trial, the spectral efficiency of a link placed in the center-most cell was collected and averaged. The transmit power of each wireless node was set according to (3) with $P_M = \infty$ (to simulate the sufficient power case) or $P_M = 200mW$. $G_t = 10^{-5}m^\alpha$, and $\alpha = 4$, were assumed.

Figure 9 shows results of Monte Carlo simulations and the asymptotic expression given by (31) for systems with unlimited transmit powers per node. Note that the simulations match the asymptotic results to within 10% when $N \geq 9$ for a relative base-station to wireless-node density of 20%. For lower relative densities, the convergence is slower. For 10% relative density, the simulations match the asymptotic expression to within 10% only when $N \geq 20$ and only when $N \geq 37$ for 5% relative density. The rate of convergence for random cells is slower than that for hexagonal cells because the range of transmit powers is much larger for random cells compared to hexagonal cells which results in slower convergence, as explained in Section V-A. Figure 10 shows simulations of systems with a 200 mW transmit power limit.

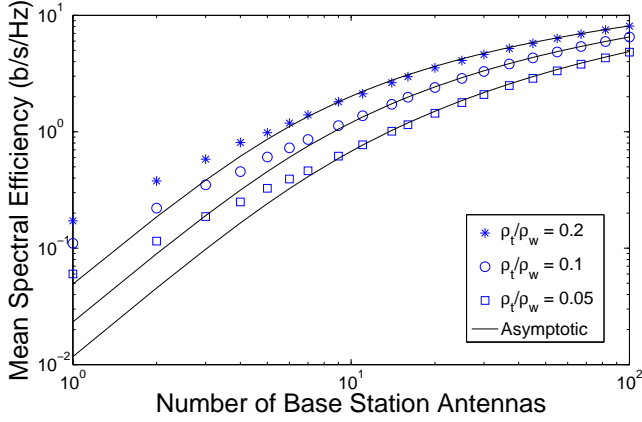


Fig. 10. Area-averaged spectral efficiency of uplink communications with random cells and 200mW transmit power limit per node. Wireless-node density $\rho_w = 10^{-3}$ nodes / m^2 , $p_t = 10^{-14}$ and $G_t = 10^{-5}$.

The target received power $p_t = 10^{-12}$. For relative base-station to wireless-node densities of 20%, 10%, and 5%, the simulated area-averaged spectral efficiencies are within 10% of the asymptotic prediction when $N \geq 6$, $N \geq 9$ and $N \geq 9$ respectively. The convergence of the simulated area-averaged spectral efficiencies to the asymptotic values is faster for systems with limited transmit power as the range of transmit powers in the network is smaller when there is a bound on the transmit power.

VI. SUMMARY AND CONCLUSIONS

We have derived an asymptotic expression for the area-averaged spectral efficiency of the uplink in wireless networks with multi-antenna base-stations in networks with hexagonal cells, a model which is known to be difficult to analyze and is typically handled in simulation. We extended the results to networks where base stations are distributed according to a Poisson point process on the plane and derive an expression for the area-averaged spectral efficiency of a random link where the averaging is over the fading, and spatial distributions of the wireless nodes and base stations. We assumed a power control algorithm for which interferers try to achieve a target received power at the base stations to which they are connected. This power control algorithm which has also been used in [8] and related works ensures that uplink spectral efficiencies are close to the average value with high probability when the number of antennas per link is large and the interferers have high power budgets.

It is found that if the cell sizes are small enough that all interferers are able to achieve the target received signal power at their base stations (which we call the sufficient-power case), the area-averaged spectral efficiency takes a simple form given by (19). Note that for a fixed ratio of base-station to wireless-node densities ρ_t/ρ_w , as ρ_w increases, the system eventually moves to the sufficient-power case so this is an effective way of scaling the density of such networks.

From (19), note that with 7 antenna elements per base station and $\rho_t/\rho_w \approx 0.1$, the area-averaged spectral efficiency

is approximately $1 \text{ bs}^{-1} \text{ Hz}^{-1}$. If we assume that 10% of all interferers are actively transmitting at any one time, the ratio of base station to total wireless-node density has to be just 1% to achieve a area-averaged spectral efficiency of $1 \text{ bs}^{-1} \text{ Hz}^{-1}$, as given by (19). For systems with insufficient power, i.e., the cells are so large that not all of the interferers will achieve the target received power at their base stations, the expression for the area-averaged spectral efficiency is more complicated and has to be evaluated by numerically. We verified the accuracy of the derived expressions by Monte Carlo simulations which were also used to study the outage spectral efficiency, i.e., the spectral efficiency that is achievable with a given probability. We found that in the sufficient power case, with 14 antennas per base station and single antennas at each wireless-node, and with 10% of interferers *transmitting simultaneously* at any one time, over $1 \text{ bs}^{-1} \text{ Hz}^{-1}$ is achievable by 95% of interferers when the ratio of base-station to active wireless-node densities is 1%.

Comparing the area-averaged spectral efficiencies for hexagonal and Poisson cells, we find that the difference in area-averaged spectral efficiency between the two models diminishes with increasing N . At modest N we found that hexagonal cells can increase the area-averaged spectral efficiency over random cells several-fold as illustrated in Figure 3.

The findings of this work are useful for designers of cellular wireless systems such as pico-cells and city-wide wi-fi access as they provide simple expressions for the spectral efficiency and hence data rates as a function of tangible system parameters such as user and base-station densities, number of base-station antennas and random versus regular distribution of base stations.

VII. ACKNOWLEDGEMENT

We would like to thank the anonymous reviewers for their comments which have greatly improved our exposition and the positioning of our results with respect to existing literature.

APPENDIX

A. Proof of Theorem 1

To derive the normalized SIR β_N , we first modify the system model from Section II. We assume that the i -th wireless-node transmits with power $\tilde{P}_i = N^{\frac{\alpha}{2}} P_i$ for $i = 2, 3, \dots, n+1$, where P_i is as defined in Section II, whereas the representative transmitter transmits with power P_1 . Thus, the SIR of this system, is equivalent to $N^{-\frac{\alpha}{2}}$ times the SIR of the original system in Section II where the interferers transmit with power P_i . Let the matrix $\mathbf{P} = \text{diag}(\tilde{P}_2 r_2^{-\alpha}, \tilde{P}_3 r_3^{-\alpha}, \dots, \tilde{P}_{n+1} r_{n+1}^{-\alpha})$. The SIR of this system normalized by p_1 is

$$\beta_N = \frac{1}{N} \mathbf{g}_1^\dagger \left(\frac{1}{N} \mathbf{G} \mathbf{P} \mathbf{G}^\dagger \right)^{-1} \mathbf{g}_1 \quad (34)$$

where \mathbf{G} is a matrix whose i -th column is \mathbf{g}_{i+1} . Note that (5) and (34) are equal.

Observe that (34) and (8) in Lemma 1 take the same form if the e.d.f. of the diagonal entries of \mathbf{P} converges *w.p.1* to a limiting function $H(x)$ as N and $n \rightarrow \infty$, and there exists an N_0 such that for all $N > N_0$, the eigenvalues of $\frac{1}{N} \mathbf{G} \mathbf{P} \mathbf{G}^\dagger$

are bounded from below. The latter requirement is satisfied as shown in the following lemma.

Lemma 5: Let $\lambda_{\min}(\mathbf{A})$ denote the minimum eigenvalue of the matrix \mathbf{A} . Consider the matrix

$$\mathbf{K} = \frac{1}{N} \mathbf{G} \mathbf{P} \mathbf{G}^\dagger = N^{\frac{\alpha}{2}-1} \sum_{i=2}^{n+1} p_i \mathbf{g}_i \mathbf{g}_i^\dagger. \quad (35)$$

Then $0 < \lambda_{\ell b} < \lambda_{\min}(\mathbf{K})$, *w.p.1* for some $\lambda_{\ell b}$ and $\forall n > N_0$ where N_0 is a positive integer.

Proof: Please see Appendix D

Hence, what remains is to show the convergence of the e.d.f. of the received interference powers. Recall that n interferers are distributed in a disk of radius R centered at the origin. Setting $G_i = 1$ for notational convenience (it will be reintroduced in the final expressions) and $\tilde{p}_i = \tilde{P}_i r_i^{-\alpha}$, the CDF of the received power from wireless-node i is

$$\begin{aligned} \Pr\{\tilde{p}_i \leq x\} &= \Pr\{P_i N^{\frac{\alpha}{2}} r_i^{-\alpha} \leq x\} \\ &= \int \Pr\left\{\frac{r_i}{\sqrt{N}} \geq \left(\frac{P_i}{x}\right)^{\frac{1}{\alpha}} \middle| P_i\right\} f_P^N(P_i) dP_i, \end{aligned} \quad (36)$$

where $f_P^N(P_i)$ is the PDF of P_i for a finite N .

Next, we use the following lemma which is proved in Appendix E

Lemma 6: For both the hexagonal-cell and Poisson-cell models, as $n, N, R \rightarrow \infty$,

$$\begin{aligned} \Pr\left\{\frac{r_i}{\sqrt{N}} \geq \left(\frac{P_i}{x}\right)^{\frac{1}{\alpha}}, P_i\right\} \rightarrow \\ \left[\left(1 - \frac{\pi \rho_w}{c} \left(\frac{P_i}{x}\right)^{\frac{2}{\alpha}}\right) I_{\left\{P_i \left(\frac{\pi \rho_w}{c}\right)^{\frac{\alpha}{2}} < x\right\}} \right] f_P(P_i). \end{aligned} \quad (37)$$

(37) indicates that the transmit power of a node randomly distributed with uniform probability in the circular network to be asymptotically independent of its normalized distance from the origin as the quantity in the brackets in (37) equals the probability that r_i/\sqrt{N} exceeds $(P_i/x)^{\frac{1}{\alpha}}$. From (36), Lemma 6, and the bounded convergence theorem, as $n, N, R \rightarrow \infty$ in the manner of Lemma 6,

$$\Pr\{\tilde{p}_i \leq x\} \rightarrow \int f_P(P) \left(1 - \frac{\pi \rho_w}{c} \left(\frac{P}{x}\right)^{\frac{2}{\alpha}}\right) I_{\{P < \frac{x}{\pi \rho_w}\}} dP \quad (38)$$

$$\begin{aligned} &= F_P\left(\frac{x}{b}\right) - \frac{\pi \rho_w}{c} x^{-\frac{2}{\alpha}} E\left[P^{\frac{2}{\alpha}}\right] \\ &\quad + \frac{\pi \rho_w}{c} x^{-\frac{2}{\alpha}} \int_{\frac{x}{b}}^{\infty} f_P(P) P^{\frac{2}{\alpha}} dP. \end{aligned} \quad (39)$$

(36) to (38) follows from (37), and from substituting $b = \left(\frac{\pi \rho_w}{c}\right)^{\frac{\alpha}{2}}$.

By the Glivenko-Cantelli theorem, the e.d.f. of a set of i.i.d. random variables converges uniformly, *w.p.1*, to its CDF. The deviation of this e.d.f. from the CDF can be bounded by an exponentially decreasing function of n , independent of the CDF [27]. Hence, by the Borel Cantelli Lemma, the e.d.f. of the \tilde{p}_i s converges *w.p.1* to the RHS of (39), i.e. $H(x) = \Pr\{\tilde{p}_i < x\}$, even though the CDF is dependent on

n . Taking the derivative of the RHS of (39) and simplifying yields:

$$\begin{aligned} \frac{dH(x)}{dx} &= \frac{2\pi \rho_w}{c\alpha} E\left[P^{\frac{2}{\alpha}}\right] x^{-\frac{2}{\alpha}-1} \\ &\quad - \frac{2\pi \rho_w}{c\alpha} x^{-\frac{2}{\alpha}-1} \int_{x/b}^{\infty} f_P(\tau) \tau^{\frac{2}{\alpha}} d\tau. \end{aligned} \quad (40)$$

Substituting (40) and integrating, the RHS of (9) becomes

$$\begin{aligned} mc \int_b^{\infty} \frac{\tau dH(\tau)}{1 + m\tau} &= mc \int_0^{\infty} \frac{2\pi \rho_w}{c\alpha} E\left[P^{\frac{2}{\alpha}}\right] \frac{\tau^{-\frac{2}{\alpha}}}{1 + m\tau} d\tau \\ &\quad - \frac{2\pi \rho_w m}{\alpha} \int_0^{\infty} \frac{\tau^{-\frac{2}{\alpha}}}{1 + m\tau} d\tau \int_{\tau/b}^{\infty} f_P(x) x^{\frac{2}{\alpha}} dx \\ &= \frac{2\pi \rho_w}{\alpha} E\left[P^{\frac{2}{\alpha}}\right] m^{\frac{2}{\alpha}} \pi \csc\left(\frac{2\pi}{\alpha}\right) \\ &\quad - \frac{2\pi \rho_w m}{\alpha} \int_0^{\infty} \frac{\tau^{-\frac{2}{\alpha}}}{1 + m\tau} d\tau \int_{\tau/b}^{\infty} f_P(x) x^{\frac{2}{\alpha}} dx. \end{aligned} \quad (41)$$

Substituting (41) into (9) completes the proof.

B. Proof of Lemma 1

The proof mirrors that of the proof of Lemma 4.3 in [19] but since the noise power is neglected in our model, a modified version of the proof is required. Let $\lambda_1, \lambda_2, \dots, \lambda_N$ denote the eigenvalues of \mathbf{R} , and perform an eigen decomposition of \mathbf{R} such that $\mathbf{R} = \mathbf{U}^\dagger \mathbf{\Lambda} \mathbf{U}$. Denoting the i -th entry of the vector \mathbf{U} s by u_i , we have

$$\gamma_N = \frac{1}{N} \sum_{i=1}^N \frac{|u_i|^2}{\lambda_i}, \quad (42)$$

which is finite *w.p.1* for $N > N_0$ since $\lambda_{\ell b} < \lambda_i$. Note that as $n, N \rightarrow \infty$, the e.d.f. of the eigenvalues of \mathbf{R} , $\Psi_N(\lambda)$, converges with probability 1 to a limiting probability distribution $\Psi(\lambda)$ [28].

For any $N > N_0$, set a $\delta_1 > 0$ and pick a finite partition of the range $(\lambda_{\ell b}, \infty)$ into M intervals (I_1, I_2, \dots, I_M) such that

$$\sum_{k=1}^M \frac{\Psi(I_k)}{I_k^l} - \int_0^{\infty} \frac{1}{\lambda} d\Psi(\lambda) < \delta_1, \quad \text{and} \quad (43)$$

$$\int_0^{\infty} \frac{1}{\lambda} d\Psi(\lambda) - \sum_{k=1}^M \frac{\Psi(I_k)}{I_k^r} < \delta_1, \quad (44)$$

where $\Psi(I_k)$ is the probability that a random variable with CDF $\Psi(\cdot)$ is in the interval I_k , and I_k^l and I_k^r are the left and right edge of the interval I_k . Consider the events

$$E_1 = \left\{ \left| \sum_{i: \lambda_i \in I_k} u_i^2 - \Psi_N(I_k) \right| < \frac{\delta_2}{M}, \forall k = 1, \dots, M \right\} \quad \text{and} \quad (45)$$

$$E_2 = \left\{ |\Psi_N(I_k) - \Psi(I_k)| < \frac{\delta_2}{M}, \forall k = 1, \dots, M \right\} \quad (46)$$

where $\Psi_N(I_k)$ denotes the probability that a random variable with CDF $\Psi_N(\cdot)$ is in the interval I_k . If both E_1 and E_2 hold, and $\sigma^2 = 0$, following [19], we have the following *w.p.1*.

$$\gamma_N \leq \sum_{k=1}^M \frac{\Psi(I_k) + 2\frac{\delta_2}{M}}{I_k^l} \leq \int_0^{\infty} \frac{1}{\lambda} d\Psi(\lambda) + \delta_1 + 2\frac{\delta_2}{\lambda_{\ell b}}, \quad (47)$$

where recall that the left-edge of the first partition $I_1^l = \lambda_{\ell b}$. Similarly we can show that $w.p.1$,

$$\gamma_N \geq \int_0^\infty \frac{1}{\lambda} d\Psi(\lambda) - \delta_1 - 2\frac{\delta_2}{\lambda_{\ell b}}. \quad (48)$$

Note that (47) and (48) are similar in form to corresponding expressions in [19] except that the noise power σ^2 in [19] is replaced with $\lambda_{\ell b}$. The remainder of the proof is identical to the proof of Lemma 4.3 in [19] with σ^2 replaced by $\lambda_{\ell b}$.

C. Proof of Lemma 4

To find $f_{P|\Pi_t}(P|\Pi_t)$, let Ξ_v be the union of the set of disks of radius v centered at each of the base stations. Thus, for $x \leq P_M$, we have

$$\Pr(P_i \leq x|\Pi_t) = \Pr(i\text{-th wireless-node} \in \Xi_v|\Pi_t) \quad (49)$$

with $v = \left(\frac{xG_t}{p_t}\right)^{1/\alpha}$. The set $\Xi_v \setminus B(0, v)$ forms a Boolean model with radius v disks as the primary grains (see Chapter 3 of [18]). The fractional area of the plane occupied by $\Xi_v \setminus B(0, v)$ equals $1 - e^{-\rho_t \pi v^2}$ *w.p.1.* [18]. Since $\Pr(i\text{-th wireless-node} \in B(0, v) = 0)$, we have for $x \leq P_M$,

$$\Pr(P_i \leq x|\Pi_t) = 1 - e^{-\rho_t \pi \left(\frac{xG_t}{p_t}\right)^{\frac{2}{\alpha}}} \quad (50)$$

and $\Pr(P_i \leq x|\Pi_t) = 1$ if $x > P_M$. Taking the derivative with respect to x yields (26). Taking the integral $\int_0^\infty p^{\frac{2}{\alpha}} f_{P|\Pi_t}(p|\Pi_t) dp$ using (26) yields (25). When conditioned on r_1 , the result still holds by the mixing property of the Poisson Voronoi tessellation (e.g. see [?]).

D. Proof of Lemma 5

Recall that $p_i = P_i G_t r_i^{-\alpha}$, and for $r_c > 0$ defined subsequently, write the matrix

$$\begin{aligned} \mathbf{K} &= N^{\frac{\alpha}{2}-1} \sum_{i=2}^{n+1} p_i \mathbf{g}_i \mathbf{g}_i^\dagger \\ &= \frac{1}{N} \sum_{i \in \mathcal{I}} N^{\frac{\alpha}{2}} P_i G_t r_i^{-\alpha} \mathbf{g}_i \mathbf{g}_i^\dagger + \frac{1}{N} \sum_{i \in \mathcal{I}^c} N^{\frac{\alpha}{2}} P_i G_t r_i^{-\alpha} \mathbf{g}_i \mathbf{g}_i^\dagger \\ &= \frac{1}{N} \sum_{i \in \mathcal{I}} N^{\frac{\alpha}{2}} \min\left(\frac{p_t r_c^\alpha}{G_t}, P_M\right) R^{-\alpha} G_t \mathbf{g}_i \mathbf{g}_i^\dagger \\ &\quad + \frac{1}{N} \sum_{i \in \mathcal{I}} N^{\frac{\alpha}{2}} \left(P_i r_i^{-\alpha} - \min\left(\frac{p_t r_c^\alpha}{G_t}, P_M\right) R^{-\alpha}\right) G_t \mathbf{g}_i \mathbf{g}_i^\dagger \\ &\quad + \frac{1}{N} \sum_{i \in \mathcal{I}^c} N^{\frac{\alpha}{2}} P_i G_t r_i^{-\alpha} \mathbf{g}_i \mathbf{g}_i^\dagger \\ &= \frac{1}{N} \sum_{i \in \mathcal{I}} \left(\frac{\pi \rho_t}{c}\right)^\alpha \min\left(\frac{p_t r_c^\alpha}{G_t}, P_M\right) G_t \mathbf{g}_i \mathbf{g}_i^\dagger \\ &\quad + \frac{1}{N} \sum_{i \in \mathcal{I}} N^{\frac{\alpha}{2}} \left(P_i r_i^{-\alpha} - \min\left(\frac{p_t r_c^\alpha}{G_t}, P_M\right) R^{-\alpha}\right) G_t \mathbf{g}_i \mathbf{g}_i^\dagger \\ &\quad + \frac{1}{N} \sum_{i \in \mathcal{I}^c} N^{\frac{\alpha}{2}} P_i G_t r_i^{-\alpha} \mathbf{g}_i \mathbf{g}_i^\dagger. \end{aligned} \quad (51)$$

$$+ \frac{1}{N} \sum_{i \in \mathcal{I}^c} N^{\frac{\alpha}{2}} P_i G_t r_i^{-\alpha} \mathbf{g}_i \mathbf{g}_i^\dagger. \quad (52)$$

where $\mathcal{I} = \{i : r_{ti} < r_c, 1 < i \leq n+1\}$ is the set of interferers that are closer than r_c to their closest base-stations.

$\mathcal{I}^c = \{i : r_{ti} \geq r_c, 1 < i \leq n+1\}$ is the set of remaining interferers. The step from (51) to (52) is from substituting $c = n/N$ and (1).

For the hexagonal-cell model, with A_H denoting the area of each hexagonal cell, $r_c = \sqrt{A_H/(2\pi)}$. For the Poisson-cell model, $r_c = \sqrt{\ln 2(\rho_t \pi)}$. These values are selected such that if we place disks of radius r_c around each base-station, the fractional area occupied by the union of these disks is $\frac{1}{2}$, exactly for the hexagonal-cell model, and *w.p.1* for the Poisson-cell model (see Chapter 3 of [18]). Thus, as $n, N, R \rightarrow \infty$, with probability approaching 1, $\frac{1}{N}|\mathcal{I}| \rightarrow c/2$ and $\frac{1}{N}|\mathcal{I}^c| \rightarrow c/2$. Let the first term on the RHS of (52) be denoted by $\mathbf{T}_1 \in \mathbb{C}^{N \times N}$. Note from the system model that $r_i \leq R$ and $P_i r_i^{-\alpha} - \min\left(\frac{p_t r_c^\alpha}{G_t}, P_M\right) R^{-\alpha} > 0$ for $i \in \mathcal{I}$ and R sufficiently large. From (52) and Weyl's inequality (see e.g., [29]), $\lambda_{\min}(\mathbf{K}) \geq \lambda_{\min}(\mathbf{T}_1)$. Additionally, from [30], as $n, N \rightarrow \infty$ such that $n/N \rightarrow c/2$,

$$\begin{aligned} \lambda_{\min}(\mathbf{T}_1) &\rightarrow \bar{\lambda}_{\min}(\mathbf{T}_1) \\ &= \left(\frac{\pi \rho_t}{c}\right)^\alpha G_t \min\left(\frac{p_t r_c^\alpha}{G_t}, P_M\right) (1 - \sqrt{2/c})^2 \text{ w.p.1.} \end{aligned}$$

Hence, as $n, N, R \rightarrow \infty$, *w.p.1*, the limiting e.d.f. of the eigenvalues of \mathbf{K} has support that is bounded from below by a non-negative number $\lambda_{\ell b}$. Note that $\lambda_{\ell b}$ could equal $\frac{1}{2} \bar{\lambda}_{\min}(\mathbf{T}_1)$ for example. Additionally, from [26] for sufficiently large N , *w.p.1*, no eigenvalues of the matrix \mathbf{K} occur outside the support of the limiting e.d.f. of the eigenvalues of \mathbf{K} . Hence, for N sufficiently large, there are no eigenvalues of \mathbf{K} that are less than $\lambda_{\ell b} > 0$ *w.p.1*.

E. Proof of Lemma 6

Here, we show that r_i/\sqrt{N} and P_i are asymptotically independent for both hexagonal and Poisson cells. Recall that node i is distributed with uniform probability in the radius R circular network and r_i , r_{ti} and P_i are its distance to the origin, distance to its closest base station and transmit power respectively, and Ξ_v is the union of the set of disks of radius v centered at the base stations. Conditioned on $r_i \leq y\sqrt{N}$, node- i is uniformly distributed in $B(0, y\sqrt{N})$. Hence,

$$\begin{aligned} \Pr\left\{r_{ti} \leq v \mid \frac{r_i}{\sqrt{N}} \leq y\right\} &= \Pr\left\{r_{ti} \leq v \mid r_i \leq y\sqrt{N}\right\} \\ &= \frac{\text{Area}\left(\Xi_v \cap B(0, y\sqrt{N})\right)}{\pi y^2 N} \end{aligned} \quad (53)$$

For hexagonal cells, as N and $R \rightarrow \infty$, the RHS approaches $F_X(v)$ from (17) as the edge effects diminish. For Poisson cells, the set $\Xi_v \setminus B(0, v)$ forms a Boolean model and as $N \rightarrow \infty$, the RHS of (53) converges to $1 - e^{-\rho_t \pi v^2}$ *w.p.1* (see Chapter 3 of [18]). Hence, r_{ti} and r_i/\sqrt{N} are asymptotically independent and since P_i is a function of r_{ti} , P_i is asymptotically independent of r_i/\sqrt{N} . Thus, as $N \rightarrow \infty$, with

probability approaching unity,

$$\Pr \left\{ \frac{r_i}{\sqrt{N}} \geq \left(\frac{P_i}{x} \right)^{\frac{1}{\alpha}} \middle| P_i \right\} \rightarrow \Pr \left\{ \frac{r_i}{\sqrt{N}} \geq \left(\frac{P_i}{x} \right)^{\frac{1}{\alpha}} \right\} \\ = \frac{R^2 - N \left(\frac{P_i}{x} \right)^{\frac{2}{\alpha}}}{R^2} I_{\left\{ 0 < \left(\frac{P_i}{x} \right)^{-\frac{1}{\alpha}} \sqrt{N} < R \right\}}.$$

Note that the RHS is simply the CDF of r_i evaluated at $\sqrt{N} \left(\frac{P_i}{x} \right)^{\frac{1}{\alpha}}$. Substituting $c = n/N$, (1), Bayes' rule, and rearranging terms in the RHS of the last equation yields (37).

REFERENCES

- [1] J. G. Andrews, F. Baccelli, and R. K. Ganti, "A tractable approach to coverage and rate in cellular networks," *IEEE Trans. Commun.*, vol. 59, no. 11, pp. 3122–3134, Apr. 2011.
- [2] H. Dai and H. V. Poor, "Asymptotic spectral efficiency of multicell MIMO systems with frequency-flat fading," *IEEE Trans. Signal Process.*, vol. 51, no. 11, pp. 2976–2988, Nov. 2003.
- [3] R. Couillet, M. Debbah, and J. Silverstein, "A deterministic equivalent for the analysis of correlated MIMO multiple access channels," *IEEE Trans. Inf. Theory*, vol. 57, no. 6, pp. 3493–3514, Jun. 2011.
- [4] D. Aktas, M. N. Bacha, J. S. Evans, and S. V. Hanly, "Scaling results on the sum capacity of cellular networks with MIMO links," *IEEE Trans. Inf. Theory*, vol. 52, no. 7, pp. 3264–3274, Jul. 2006.
- [5] S. Catreux, P. F. Driessen, and L. J. Greenstein, "Simulation results for an interference-limited multiple-input multiple-output cellular system," *IEEE Commun. Lett.*, vol. 4, pp. 334–336, Nov. 2000.
- [6] C. C. Chan and S. V. Hanly, "Calculating the outage probability in a CDMA network with spatial Poisson traffic," *IEEE Trans. Veh. Technol.*, vol. 50, pp. 183–204, Jan. 2001.
- [7] T. D. Novlan, H. S. Dhillon, and J. G. Andrews, "Analytical modeling of uplink cellular networks," *CoRR*, vol. abs/1203.1304, 2012.
- [8] S. Weber, X. Yang, J. G. Andrews, and G. de Veciana, "Transmission capacity of wireless ad hoc networks with outage constraints," *IEEE Trans. Inf. Theory*, vol. 51, no. 12, pp. 4091–4102, Dec. 2005.
- [9] S. Govindasamy, F. Antic, D. W. Bliss, and D. Staelin, "The performance of linear multiple-antenna receivers with interferers distributed on a plane," *Proc. IEEE SPAWC*, 2005.
- [10] S. Govindasamy, D. W. Bliss, and D. H. Staelin, "Spectral efficiency in single-hop ad hoc wireless networks with interference using adaptive antenna arrays," *IEEE J. Sel. Areas Commun.*, vol. 25, no. 7, pp. 1358–1369, Sep. 2007.
- [11] N. Jindal, J. Andrews, and S. Weber, "Multi-antenna communication in ad hoc networks: Achieving MIMO gains with SIMO transmission," *IEEE Trans. Commun.*, vol. 59, no. 2, pp. 529–540, Feb. 2011.
- [12] O. Ali, C. Cardinal, and F. Gagnon, "Performance of optimum combining in a Poisson field of interferers and Rayleigh fading channels," *IEEE Trans. Wireless Commun.*, vol. 9, no. 8, pp. 2461–2467, Aug. 2010.
- [13] R. Louie, M. McKay, and I. Collings, "Open-loop spatial multiplexing and diversity communications in ad hoc networks," *IEEE Trans. Inf. Theory*, vol. 57, no. 1, pp. 317–344, Jan. 2011.
- [14] M. Haenggi, J. G. Andrews, F. Baccelli, O. Dousse, and M. Franceschetti, "Stochastic geometry and random graphs for the analysis and design of wireless networks," *IEEE J. Sel. Areas Commun.*, vol. 27, no. 7, pp. 1029–1046, Sep. 2009.
- [15] F. Baccelli and B. Błaszczyszyn, *Stochastic Geometry and Wireless Networks, Volume II - Applications*, ser. Foundations and Trends in Networking: Vol. 4: No 1-2, pp 1-312. NoW Publishers, 2009, vol. 2.
- [16] —, *Stochastic Geometry and Wireless Networks, Volume I - Theory*, ser. Foundations and Trends in Networking Vol. 3: No 3-4, pp 249-449. NoW Publishers, 2009, vol. 1.
- [17] W. Xiao, R. Ratasuk, A. Ghosh, R. Love, Y. Sun, and R. Nory, "Uplink power control, interference coordination and resource allocation for 3GPP E-UTRA," in *Proc. IEEE Vehicular Technology Conference*, Sep. 2006, pp. 1–5.
- [18] D. Stoyan, W. S. Kendall, and J. Mecke, *Stochastic Geometry and Its Applications*. John Wiley and Sons, 1995.
- [19] D. Tse and S. Hanly, "Linear multiuser receivers: Effective interference, effective bandwidth and user capacity," *IEEE Trans. Inf. Theory*, vol. 45, no. 2, pp. 641–657, Mar. 1999.
- [20] K. Gulati, B. Evans, J. Andrews, and K. Tinsley, "Statistics of co-channel interference in a field of Poisson and Poisson-Poisson clustered interferers," *IEEE Trans. Signal Process.*, vol. 58, no. 12, pp. 6207–6222, Dec. 2010.
- [21] Z. Bai and J. W. Silverstein, "On the signal-to-interference-ratio of CDMA systems in wireless communications," *Annals of Applied Probability*, vol. 17, no. 1, pp. 81–101, 2007.
- [22] A. F. Karr, *Probability*. Springer-Verlag, 1993.
- [23] S. Govindasamy, D. W. Bliss, and D. H. Staelin, "Asymptotic spectral efficiency of multi-antenna links in wireless networks with limited Tx CSI," *IEEE Trans. Inf. Theory*, Sept. 2012.
- [24] A. M. Mathai, *An Introduction to Geometrical Probability*. Gordon and Breach Science Publishers, 1999.
- [25] P. Pirenen, "Cellular topology and outage evaluation for DS-UWB system with correlated lognormal multipath fading," *The 17th Annual IEEE International Symposium on Personal, Indoor and Mobile Radio Communications*, 2006.
- [26] Z. D. Bai and J. W. Silverstein, "No eigenvalues outside the support of the limiting spectral distribution of large-dimensional sample covariance matrices," *Ann. Probab.*, vol. 26, no. 1, pp. 316–345, 1998.
- [27] A. Dvoretzky, J. Kiefer, and J. Wolfowitz, "Asymptotic minimax character of the sample distribution function and of the classical multinomial estimator," *The Annals of Mathematical Statistics*, vol. 27, no. 3, pp. 642–669, 1956.
- [28] Z. D. Bai and J. Silverstein, "On the empirical distribution of eigenvalues of a class of large dimensional random matrices," *Journal of Multivariate Analysis*, vol. 54, pp. 175–192, 1995.
- [29] R. Horn and C. R. Johnson, *Matrix Analysis*. Cambridge University Press, 1990.
- [30] Z. D. Bai and Y. Q. Yin, "Limit of the smallest eigenvalue of a large dimensional sample covariance matrix," *Ann. Probab.*, vol. 21, pp. 1275–1294, 1993.